Appl. Phys. B 37, 181–187 (1985)

Applied Physics B Photophysics and Laser Chemistry



# Holographic Storage in Sensitized Polymethyl Methacrylate Blocks

J. Marotz

Universität Osnabrück, FB Physik, D-4500 Osnabrück, Fed. Rep. Germany

Received July 25, 1984/Accepted April 24, 1985

**Abstract.** The storage properties of thick PMMA-blocks, sensitized for $\lambda = 514\,\text{nm}$ and containing residual monomer, are investigated by making use of holographic methods. The fundamental refractive index grating amplitude shows a characteristic development in a two-beam holographic experiment. A remarkable self-development of the light induced refractive index change is observed just as considerable higher harmonic amplitudes (strong nonlinear response). The recording-sensitivity is small in comparison to that of other storage materials and adversely affected by appreciable holographic scattering. The behavior of the samples during long storage times is investigated and the possibility of thermal fixing and superposition of holograms is shown. The interpretation of the observed properties and the behavior in the holographic experiments suggests a model of the microscopic processes: storage is essentially performed by light induced polymerisation of residual monomer.

**PACS:** 42.40, 82.35

## Introduction

Holographic information storage by volume-phase-holography is of particular interest because of the extremely high storage density, which can be achieved by this method.

Photopolymers have been proved to be usable for optical data stores working on the base of volume-phase-holography as for many other devices in integrated optics [1, 2].

Especially polymethyl methacrylate (PMMA) has been frequently investigated under varying experimental conditions [3–8]. PMMA-samples of good optical quality are relatively easy to produce and are photosensitive to uv-light. Furthermore it has been shown, that the photosensitivity can be shifted to regions of larger wavelength by doping the samples with photoinitiators [4, 5]. Depending on the experimental conditions different mechanisms be responsible for the storage, among them cross-linking of the polymer matrix and light induced polymerisation of residual monomer.

In this contribution the storage properties of thick PMMA-blocks ($0.5 \leqq d \leqq 3\,\text{mm}$), sensitized for $\lambda = 514\,\text{nm}$ and containing residual monomer, are investigated by making use of the holographic method. Special attention is paid to the underlying microscopic processes. We want to utilize the large monomer content of our PMMA-blocks for light induced polymerisation which leads to an increasing density and so to refractive index changes.

To start the polymerisation with visible light, we add titanium-biscyclopentadienyl-dichloride (titanocene chloride) as photoinitiator. The absorption spectrum (Fig. 1) elucidates the advantage of this photoinitiator for the use of the 514 nm-Ar-Laser line.

## 1. Preparation

The monomer (MMA) is prepolymerized at 50 °C using azobisisobutyronitril (AIBN) as initiator. To obtain thick blocks of good optical quality, the prepolymerisation is performed between two glas-plates spaced and tighted by PVC-tubes of different diameter. By these means destroying of the material by volume contraction is avoided. The produced blocks exhibit a monomer content of approximately 10%

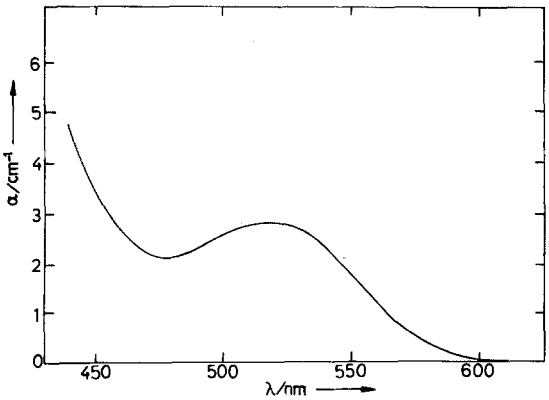


Fig. 1. Absorption spectrum of a sensitized PMMA-block (titanocenechloride-concentration: 0.5‰)

widely independent of the initiator concentration. This was established by Kopietz et al. [9, 10]. The samples are photosensitive to uv-light [9, 10]. For the experiments with green light ($\lambda = 514$ nm) titanocenechloride is added as photoinitiator at the stage of preparation of the PMMA-blocks by radical polymerisation (concentration: 0.5‰). The PMMA-blocks were produced by Kopietz as described earlier [10]. The size of the blocks used in experiment is $10\,\text{mm} \times 10\,\text{mm} \times d$ ($0.5 < d < 3\,\text{mm}$).

## 2. Experimental Set-Up

The light induced refractive index changes are investigated by holographic methods.

An intensity grating is generated by two-wave interference utilising a well-known holographic arrangement as described in the paper [6]. The two expanded beams (diameter $\approx 1.5$ mm) of an argon-ion laser interferred symmetrically at the sample (angle of incidence $\theta$ between 2 and 10°), generating a light pattern

$$I(x) = I_0 \cdot (1 + m \cdot \cos(kx)). \tag{1}$$

Here $I_0 = I_R + I_S$ ($I_0$: 20–250 mW/cm$^2$; the subscripts $R$ and $S$ denote the two beams) is the entire intensity, $m$ is the modulation index ($m = 2(I_R I_S)^{1/2}(I_R + I_S)^{-1}$) and $k = 2\pi/\Lambda$ is the spatial frequency with the fringe spacing $\Lambda = \lambda/2 \sin\theta$ ($\Lambda$ between 1.5 and 7 μm).

If the response of the material is simply linear to intensity, the light pattern produces a refractive index grating

$$n(x) = n_0 + \Delta n/2(1 + \cos(kx)). \tag{2}$$

If $\Delta n$ is small and absorption effects negligable (no absorption grating; the absorption constant $\alpha$ is not varying in $x$-direction), the diffraction efficiency $\eta$ is related to $\Delta n$ by the Kogelnik formula [11]:

$$\eta = \exp(-\alpha d/\cos\theta) \sin^2(\pi \Delta n d/\lambda \cos\theta). \tag{3}$$

The refractive index grating is illuminated with one beam only (intensity $I_E$) and $\lambda$ and $\theta$ satisfy the Bragg condition

$$2\Lambda \sin\theta = \lambda. \tag{4}$$

The diffraction efficiency $\eta$ is defined as the ratio $I_D/I_E$, where $I_D$ denotes the intensity of the diffracted beam.

If $\Delta n$ is not constant in the $z$-direction, $\Delta n$ in (3) has to be replaced by the mean value $\overline{\Delta n}$ over the sample thickness [12]. The development of the diffraction efficiency during illumination is measured by momentarily blocking one of the beams at regular intervals.

## 3. Experimental Results

### 3.1. Holographic Measurements

Because we want to use holographic methods to obtain information on the microscopic process which is responsible for the refractive index change, we must have a relation between the measured diffraction efficiency and the refractive index amplitude. The Kogelnik-formula (3) provides this relation for a pure sinusoidal grating. Generally the response of the material to the intensity is nonlinear, so that the resulting refractive index grating consists of higher harmonic gratings besides the fundamental grating. For symmetrical experimental arrangement there should not be a phase shift between the intensity grating and the resulting refractive index grating due to physical processes in PMMA and the refractive index grating can be written as a cosine series. It has been shown [13, 14], that, for small grating amplitudes, the first-order diffraction efficiency $\eta_1$ is related to the amplitude of the first harmonic grating $\Delta n_1$ by the Kogelnik-relation (3) in a good approximation.

On principle in thick samples dynamical effects must be considered. If the experimental arrangement is not symmetrical, i.e. $I_R \neq I_S$, there is a phase shift of the intensity grating during writing. Because of the irreversibility of the photoinitiation this is obviously a very disturbing effect. This can be avoided by choosing $I_R(0, t)$ and $I_S(0, t)$ to be equal.

Under these conditions we observe experimentally a diffraction efficiency development versus illumination-time over two maxima with practically $\eta = 100\%$ at the first maximum and $\eta = 0\%$ at the first minimum (Fig. 2). $\eta$ is measured with respect to the total emerging intensity, so that absorption is not considered.

In order to calculate $\Delta n_1$ from $\eta_1$ by (3), we restrict ourselves to samples, which reach saturation before the first minimum (Fig. 3). We find in all cases investigated that $\Delta n_1(t)$ shows a characteristic development:

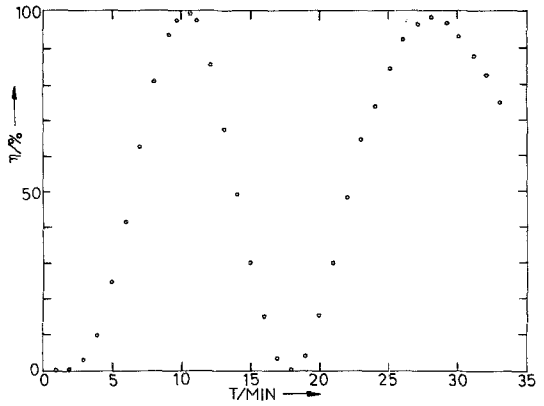


Fig. 2. Diffraction efficiency ($\eta$)-development vs. illumination time ($d=2.6$ mm, intensity $I=235\,\mathrm{mW/cm^2}$)

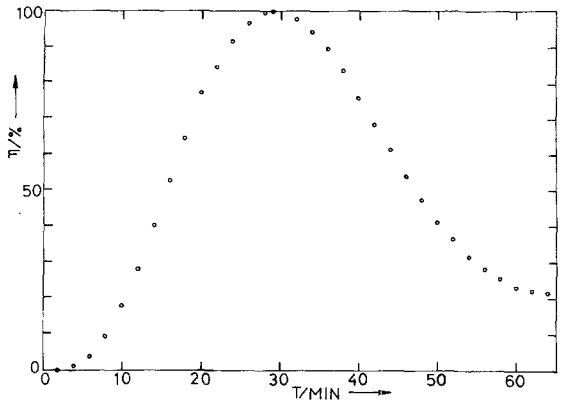


Fig. 3. $\eta$-Development vs. illumination time ($d=2.5$ mm, $I=130\,\mathrm{mW/cm^2}$)

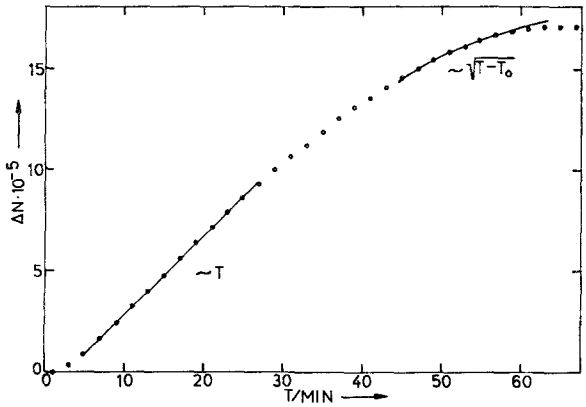


Fig. 4. Typical development of the fundamental grating amplitude $\Delta n_1(t)$ vs. illumination time ($d=2.5$ mm, $I=130\,\mathrm{mW/cm^2}$)

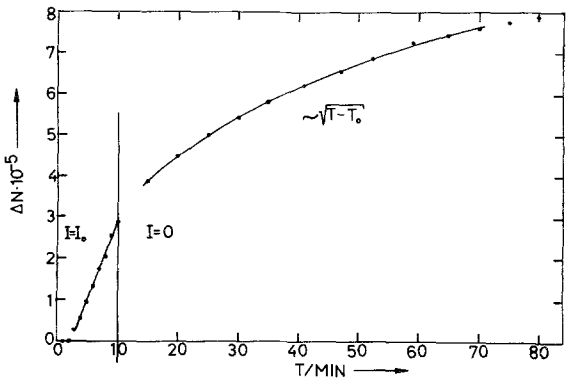


Fig. 5. $\eta$-Development; illumination is stoped at $t_S=10$ min ($d=2.5$ mm, $I=140\,\mathrm{mW/cm^2}$)

We observe a delay-time region ($T_D$) at the beginning of illumination followed by a linear growth region $\Delta n_1 \sim t$, a square root region, characterized by $\Delta n_1 \sim (t-t_0)^{1/2}$ (separated from the linear part by a transition stage) and finally the saturation region (Fig. 4). $\Delta n_1(t)$ grows up to about $3\times10^{-4}$. The absorption varies between $2.5\,\mathrm{cm^{-1}}$ at the beginning and $0.7\,\mathrm{cm^{-1}}$ at saturation. Taking into account absorption by initiator, $\eta_1$ amounts to 75% at the maximum in samples without appreciable scattering (see Sect. 3.4).

To test the applicability of (3) we additionally compare the $\Delta n_1$-growth-curves in samples of various thickness. This curves agree satisfactorally up to the square root region. But the slope of the square root dependence and the saturation value in samples with $d<1$ mm is always smaller than in samples with $d>1$ mm, for which the growth-curves agree over the whole range.

If the illumination is stopped at a time $t_S$ in the first part of the growth-curve (delay-time and linear region), the samples exhibit a remarkable self-developing of $\Delta n_1$ (Fig. 5). If the illumination is stopped in the square root region, there is no deviation from the growth with illumination. So we can roughly subdivide the growth-curve into an intensity-dependent part (delay-time, linear region) and an intensity-independent part (square root, saturation region) separated by the transition stage. To get information about the non-linearity of the material response, we analyse the higher-order diffraction efficiencies. In the saturation region we obtain considerable values for the second- and third-order diffraction efficiencies ($\eta_2, \eta_3$). The calculated corresponding amplitudes [13, 15] $\Delta n_1$, $\Delta n_2$, $\Delta n_3$ are of comparable magnitude, $\Delta n_2$ often greater than $\Delta n_1$. Figure 6 shows an example of a resulting $\Delta n(x)$-curve with $\Delta n_1=6.05\times10^{-5}$, $\Delta n_2=8.925\times10^{-5}$, $\Delta n_3=4.25\times10^{-5}$, and $\Delta n_4=0.5\times10^{-5}$ (all amplitudes are chosen to be positive), compared with the first harmonic.

### 3.2. Sensitivity

To compare our samples with other storage materials, we investigate the intensity-dependence of the first part of the growth-curve. The delay-time $T_D$ decreases asymptotically with increasing intensity down to about 15–20 s for $I=250\,\mathrm{mW/cm^2}$. The slope of the

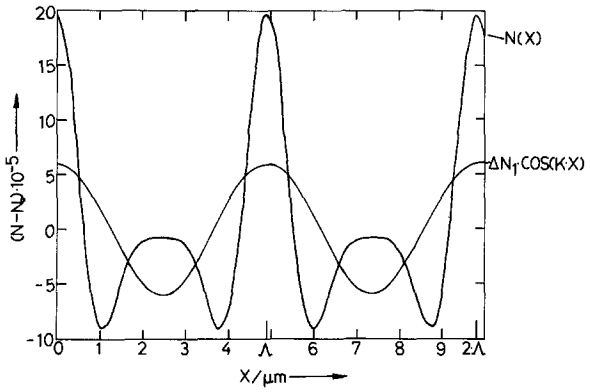


Fig. 6. Refractive index pattern of a pure cosine-grating: $n(x)-n_0 = \Delta n_1 \cos(kx)$ with $\Delta n_1 = 6.05 \times 10^{-5}$, $\Lambda = 4.93\,\mu m$ and in consideration of higher harmonics: $n(x)-n_0 = \Delta n_1 \cos(kx) + \Delta n_2 \cos(2kx) + \Delta n_3 \cos(3kx) + \Delta n_4 \cos(4kx)$ with $\Delta n_1 = 6.05 \times 10^{-5}$, $\Delta n_2 = 8.925 \times 10^{-5}$, $\Delta n_3 = 4.25 \times 10^{-5}$, $\Delta n_4 = 0.5 \times 10^{-5}$

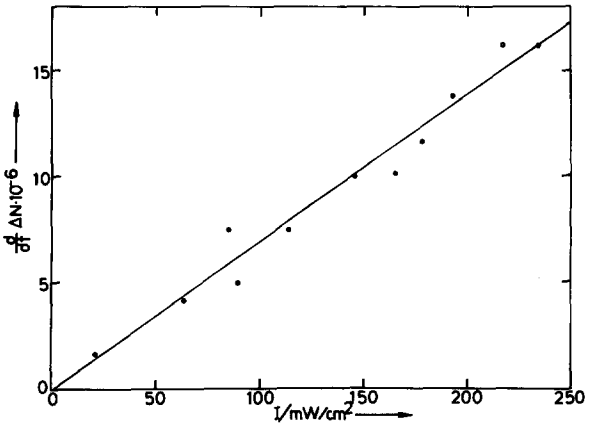


Fig. 7. Slope of the linear growth $\Delta n_1(t) \sim t$ vs. writing intensity

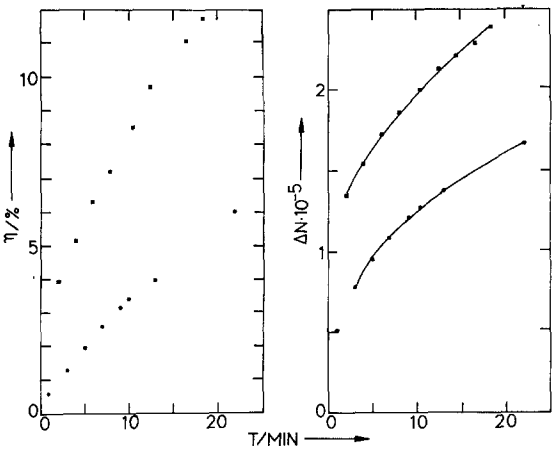


Fig. 8. $\eta$-Development (left graph) and $\Delta n$-development (right graph) after 10 (●), respectively 20 s (■) illumination ($d = 2.5$ mm, $I = 280\,mW/cm^2$)

linear growth increases linear with intensity (Fig. 7). Hence we calculate for the writing sensitivity $S = d(\Delta n)/d(I \cdot t)$ in the linear region $S \approx 6.8 \times 10^{-4}$ $cm^2/J$. Because of the inevitable delay-time and the self-developing effects, the energy density for recording a grating of 1% read out efficiency $W(1\%)$ is of more practical importance. Figure 8 shows an example for the increase of $\eta$ and $\Delta n_1$ after 10 respectively 20 s illumination time ($I = 280\,mW/cm^2$). For 10 s saturation efficiency is of the order of 5% (taking into consideration the absorption). To obtain 1% efficiency (saturation), we need ca. 2 s illumination. From this, $W(1\%)$ is estimated to $0.55\,J/cm^2$ for this sample ($d = 2.5$ mm). This value may be further optimized by higher initiator concentrations.

Furthermore the sensitivity of the material depends on the time which the samples have been stored after preparation. The samples usually have been stored in the darkness in relatively large boxes (large in comparison to the sample size) at room temperature. No decrease of absorption is observed, but the $\Delta n_1$-growth decreases in all regions with increasing storage-time. Heating up the samples at 70 °C for a few hours accelerates this process up to insensibility of the samples. In reverse, "old" samples may be regenerated by keeping them in a monomer atmosphere for a few hours.

Growing older could be widely prevented (for several month) by storing the samples in tight small bottles.

### 3.3. Thermal Fixing

Fixing may be easily carried out by heating up the samples to about 70 °C for a few hours. This procedure leads to considerable changes of the diffraction efficiency in comparison to the value at the beginning of the fixing. Even in the saturation region the corresponding refractive index amplitude $\Delta n_1$ changes up to 1.5 to 2 times by this procedure. From the great change of the diffraction efficiency through fixing, it cannot be decided, whether $\Delta n_1$ increases or decreases. Further investigations with smaller changes point to an increase of $\Delta n_1$.

Without thermal fixing the developing process of $\Delta n_1$ takes several weeks.

### 3.4. Holographic Scattering

In sufficiently thick samples ($d > 1$ mm) a characteristic light scattering appears. The scattered intensity increases during illumination up to about 30% of the writing intensity. In an experiment, where the sample is illuminated by a single beam only (wavelength $\lambda_0$, angle of incidence $\phi_0$), this scattering effects are investigated. During illumination the scattering shows a strong angle selectivity. Most of the scattered

Table 1. Experimental and theoretical (5), (6) values for the angles of the two scattering rings in a single beam experiment, measured in the plane of incidence

| $\phi-\phi_0$ [deg] | 1 | 2 | 3 | 4 | 6 | 8 | 10 |
|---|---|---|---|---|---|---|---|
| $\alpha_1$ (exp) | | 2.29 | | 4.40 | 6.60 | 8.81 | 11.07 |
| $\alpha_1$ (cal) | | 2.21 | | 4.41 | 6.62 | 8.82 | 11.04 |
| $\alpha_2$ (exp) | 10.00 | 21.00 | 32.50 | 43.50 | | | |
| $\alpha_2$ (cal) | 10.70 | 21.56 | 32.80 | 44.82 | | | |

intensity disappears if the beam is turned out of its original direction. If another laser beam (wavelength $\lambda$, angle of incidence $\phi$) impinges on those previously illuminated regions, the scattered intensity appears in two characteristical rings in a plane parallel to the surface of the sample, at first observed in PMMA by Moran and Kaminow [6]. The diameter of these rings depends on the wavelength $\lambda$ and the angle of incidence $\phi$. If $\lambda=\lambda_0$ and $\phi=\phi_0$ the rings disappear and the intensity is scattered into all directions symmetrical to the beam direction (but forward scattering is preferred). For $\lambda=\lambda_0$ and $\phi\neq\phi_0$ the diameter of the outer ring is infinite. For $\lambda\neq\lambda_0$ and $\phi\neq\phi_0$ the two rings can be observed as described in the paper [6].

This scattering is due to holograms resulting from the interference of the incident wave with waves scattered from defects near the surface [16, 17]. This effect is also known in electro-optic crystals [18].

The $\lambda$ and $\phi$-dependence can be easily derived from a construction with Ewald-spheres [16, 17]. We find for the angles $\alpha_1$ and $\alpha_2$ (measured in the plane of incidence with respect to the incident beam) under which the two rings are observed on a screen parallel to the surface of the sample:

$$\alpha_1=2\cdot(\phi-\phi_0-\arctan((1/\lambda\cdot\sin(\phi-\phi_0))/(1/\lambda_0+1/\lambda\cdot\cos(\phi-\phi_0)))), \quad (5)$$

$$\alpha_2=2\cdot(\pi/2+\phi-\phi_0-\arctan((1/\lambda_0-1/\lambda\cdot\cos(\phi-\phi_0))/(1/\lambda\cdot\sin(\phi-\phi_0)))). \quad (6)$$

Table 1 shows a comparison of calculated and measured values.

### 3.5. Holograms

Finally holograms are written in the samples by placing a transparency in one of the beams which is sufficiently expanded. The resulting holograms show a good quality before and after fixing. At higher photoinitiator concentrations (up to 3‰) the holograms become blurred during illumination and finally disappear completely. This may be due to effects connected with rising temperature in the illuminated region (strong absorption).

From an experiment, in which some holograms have been superposed in the same volume under different Bragg angles, the angular selectivity is found to be smaller than 0.3°. That means, if the sample is rotated about 0.3° out of the Bragg angle, the reconstruction is completely vanished and a new hologram can be written.

## 4. Discussion

### 4.1. Microscopic Process

The agreement of the $\Delta n$-values determined from samples of various thickness confirms the validity of (3) at least for the first part of the growth-curve (up to the transition stage). The deviation of the square root and saturation region in samples with $d<1$ mm compared to samples with $d>1$ mm may be due to chemical differences between the relative thin samples and thicker samples rather than to processes connected with the writing of the grating, because this part of the growth-curve is independent of illumination. So we can interprete our experimental results to get informations about the microscopic process.

Our results exhibit the fundamental role of the residual monomer. The marked self-developing demonstrates that refractive index change is due to increasing density caused by light induced polymerisation of the residual monomer (in contrast to cross-linking). The square root-growth points to a diffusion controlled process. Remained AIBN and evaporation of the monomer may reduce the monomer content during storage of the samples (if they are not stored in the way described in Sect. 3.2) and therefore they grow old. Heating up the material accelerates this process and so thermal fixing becomes possible.

The considerable increase of $\Delta n$ through fixing and the long-time-development without fixing (starting from the saturation value of the writing process) may indicate (slow) volume effects. But the fixing of the holograms as described in Sect. 3.5 shows, that those effects do not deteriorate essentially the quality of the stored holograms if storage is performed with moderate initiator concentration.

The $\Delta n$-growth-curve can be described by a superposition of (intensity-dependent) radicalisation of the photoinitiator and the diffusion-controlled growth of

the density due to polymerisation (intensity-independent). But it is important to notice that $\Delta n_1(t)$ only exhibits the growth of the first harmonic grating amplitude, whereas we have established also comparable amplitudes of the second and third harmonics at saturation.

A simple diffusion model can reproduce the characteristic forms of the $\Delta n_1$-growth and the refractive index grating (Figs. 4 and 6). In this model volume effects are neglected and the refractive index is assumed to be proportional to the density $\varrho$ over the corresponding region. So refractive index change is simply attributed to the change of the number of "particles" in a certain volume (i.e. free and polymerized monomer) due to diffusion of the free monomer.

We assume a simple reaction scheme:

Initiation reaction: $S+M \xrightarrow{k_S \cdot I} R$

($S$: photoinitiator, $R$: polymerradicals, $I$: intensity, $k_S$: reaction constant)

polymerisation: $R+M \xrightarrow{k_R} R$

($M$: monomer, $k_R$: reaction constant)

termination: $R \xrightarrow{k_A} P$

($P$: neutral polymers, $k_A$: reaction constant).

Taking into account the diffusion of the free monomer, differential equations can be derived, which reproduce qualitatively the characteristic forms of $\Delta n_1(t)$ and $n(x)$:

Diffusion of the monomer (one-dimensional model):

$$j(x,t) = -D \cdot \frac{dM}{dx}(x,t), \tag{7}$$

$D$: diffusion constant
$M(x,t)$: monomer distribution
$j(x,t)$: monomer current.

Hence it follows for the free monomer

$$\frac{dM}{dt}(x,t) = -\frac{dj}{dx}(x,t) - k_R \cdot R(x,t) \cdot M(x,t) \tag{8}$$

and for the distribution of polymerized monomer $M^p$:

$$\frac{dM^p}{dt}(x,t) = k_R \cdot R(x,t) \cdot M(x,t). \tag{9}$$

This leads to

$$\frac{dN}{dt}(x,t) = -\frac{dj}{dx}(x,t) \tag{10}$$

for the total number of "particles" $N = M + M^p$.

Hence the refractive index change $\Delta n(x,t)$ can be calculated from

$$\Delta n(x,t) = k_n/V \cdot \left( (M(x,t) - M_0) + k_R \int_{t_0}^{t} R(x,t) \cdot M(x,t) \cdot dt \right)$$
$$(n = k_n \cdot \varrho,\ \varrho = N/V \text{ and } V = \text{const}). \tag{11}$$

$\Delta n(x,t)$ and the first harmonic amplitude $\Delta n_1(t)$ can be easily calculated from this equations.

Because there are two superposed processes, the model elucidates that, besides the nonlinear response of the diffusion process, the distribution of the radicals is also nonlinear to the intensity pattern:

$$R(x,t) = S_0 \cdot k_S I/(k_A - k_S I(x)) \cdot (\exp(-k_S I(x)t) - \exp(-k_A t)), \tag{12}$$

where $k_A$ may be neglected in comparison to $k_S I(x)$. So the smallest nonlinearity may be obtained with relatively short illumination times, when the radical distribution is approximately linear to the intensity pattern.

This model should merely show, that this basic mechanism and assumptions are sufficient to give rise to the significantly non-linear character of the forms of $\Delta n(x)$ and $\Delta n_1(t)$. For a comparison with experiments there must be included additional effects like volume contraction and temperature dependence.

### *4.2. Storage Properties*

PMMA-blocks with good optical quality and sufficient residual monomer content are easy to produce. Holograms can be irreversibly stored in these blocks and thermally fixed. The samples containing fixed holograms need no special treatment.

Because of the relatively stable polymer radicals the self-developing reduces the required energy ($W(1\%)$) to smaller values, which are nevertheless large in comparison to that of other materials, e.g. electro-optic crystals [19].

The delay-time, together with the self-development, offers the possibility of superposing holograms in the same volume without mutually disturbances during the writing of these holograms. Nevertheless the small sensitivity and a considerable holographic scattering are surely derogatory properties.

## 5. Conclusion

Our investigation exhibits the applicability of sensitized PMMA-blocks for permanent holographic storage and yields informations about the underlying process and about storage properties. The holographic method proves to be a very powerful tool in the region of small refractive index changes.

*Acknowledgements.* The author would like to thank Prof. E. Krätzig for his support just as Dr. H. Franke for stimulating discussions and M. Kopietz for the preparation of the samples.

## References

1. W.J. Tomlinson, E.A. Chandross: Adv. in Photochem., Vol. 12, ed. by J.N. Pitts (Wiley, New York 1980) pp. 201–281
2. W.J. Tomlinson, E.A. Chandros, I.P. Kaminow, H.R. Weber, G.D. Aumiller: Appl. Opt. **15**, 534–541 (1976)
3. W.J. Tomlinson, I.P. Kaminow, E.A. Chandros, R.L. Fork, W.T. Silfrast: Appl. Phys. Lett. **16**, 486–489 (1970)
4. F.P. Laming: Polym. Eng. Sci. **11**, 421 (1972)
5. R.G. Zech: J. Opt. Soc. Am. **62**, 1396A (1972)
6. J.M. Moran, I.P. Kaminow: Appl. Opt. **12**, 1964–1970 (1973)
7. M.J. Bowden, E.A. Chandross, I.P. Kaminow: Appl. Opt. **13**, 112–117 (1974)
8. A. Bloom, R.A. Bartolini, H.A. Weaklien: Opt. Eng. **17**, 446 (1978)
9. M. Kopietz, M.D. Lechner, D.G. Steinmeier: Eur. Polym. J. **20**, 667–670 (1984)
10. M. Kopietz, J. Marotz, H. Franke, E. Krätzig, M. D. Lechner, D.G. Steinmeier: Polym. Photochem. **5**, 109–119 (1984)
11. H. Kogelnik: Bell Syst. Techn. J. **48**, 2909–2947 (1969)
12. N. Uchida: J. Opt. Soc. Am. **63**, 280–287 (1973)
13. S.F. Su, T.K. Gaylord: J. Opt. Soc. Am. **65**, 59–64 (1975)
14. R. Magnusson, T.K. Gaylord: J. Opt. Soc. Am. **67**, 1165–1170 (1977)
15. R. Alferness: J. Opt. Soc. Am. **66**, 353–362 (1976)
16. R. Magnusson, T.K. Gaylord: Appl. Opt. **13**, 1545–1548 (1974)
17. M.R.B. Forshaw: Appl. Opt. **13**, 2 (1974)
18. W. Phillips, J.J. Amodei, D.L. Staebler: RCA Rev. **33**, 94–109 (1972)
19. P. Günter: Phys. Rep. **93**, 199–299 (1982)